Simulation of biogas counter flow diffusion flame under several operation conditions of composition and pressure

A. Mameri[1,*], F. Tabet[2]and A. Hadef[1]

[1]Faculté des sciences et sciences appliquées, FSSA. Dept. du Génie Mécanique, Université Larbi Ben M'hidi, Oum El Bouaghi, BP 358 04000, Algérie

[2]DBFZ (Deutsches Biomasseforschungszentrum gemeinnützige GmbH), Torgauer Straße 116 D-04347 Leipzig, Germany.

mameriabdelbaki@yahoo.fr

Résume

Cette étude considère l'influence de plusieurs conditions opératoires (composition et pression ambiante) sur la structure de la flamme non pré mélangée du biogaz et l'émission du NO. La flamme du biogaz est modélisée par une flamme de diffusion à contre courant et analysée dans le plan de la fraction de mélange en utilisant l'approche des flammelettes. La cinétique chimique est représentée par le mécanismeGRI Mech-3.0 qui comprend 53 espèces chimiques et 325 rectionsélémentaires.

Il a été observé que l'ajout du CO2 diminue la température de la flamme, la fraction massique des radicaux O, H et OH et de l'indice d'émission de NO. Le CO2ajouté peut participer dans la réaction chimique du à la dissociation thermique; par contre l'ajout d'une quantité importante de CO2 joue le rôle d'un diluant. L'augmentation de la pressionréduit l'épaisseur de la flamme, les pertes par rayonnement et le taux de dissociation. Aux pressions élevées, les réactions de recombinaisoncouplée avec la réduction des radicaux porteurs de chaine réduit la fraction massique du NO.

Abstract

This study addresses the influence of several operating conditions (composition and ambient pressure) on biogas diffusion flame structure and NO emissions with particular attention on chemical and thermal effect of CO2.The biogas flame is modeled by a counter flowdiffusion flame and analyzed in mixture fraction space using flamelet approach. The GRI Mech-3.0 mechanism that involves 53 species and 325 reactions is adopted for the oxidation chemistry.

It has been observed that flame properties are very sensitive to biogas composition and pressure. CO2 addition decreases flame temperature, mass fraction of chain carrier radicals (O,H and OH) and index NO emission. Added CO2 may participate in chemical reaction due to thermal dissociation; excessively supplied CO2 plays the role of pure diluent. Pressure rise reduces flame thickness, radiation losses and dissociation amount. At high pressure, recombination reactions coupled with chain carrier radicals reduction, diminishes NO mass fraction.

1. Introduction

Biogas is composed (by volume) mainly of methane (CH4 : 40%-70%), carbon dioxide (CO2 : 60%-30%), smaller amount of hydrogen sulphide (H2S : 1000-5000 ppm), moistures and siloxanes. Carbon dioxide CO2 in biogas (30% to 60%) can act as a diluent which reduces heating value, laminar burning velocity, flame stability and flammability range [1].

Research activities on biogas as a fuel are performed in several configurations (laboratory flames, gas turbines, thermal combustion engines, etc.). In the following, the main results obtained are summarized.

A simulation analysis of biogas diffusion flame, using full and reduced mechanism, was conducted on blends of CH4 and CO2 by Saeed Jahangirian et al [2] to study the dioxide concentration effects on flame structure. It was shown that the reduced mechanism poorly tracks the minor species and chain branching radicals. The computations done with the full mechanism suggested that biogas may be beneficial for soot suppression.

Nathan and Stone [3] conducted an experimental study to measure the laminar flame velocity of methane/carbon dioxide with air under the following conditions: ambient pressure up to 18 bars, injection temperature up to 660 K, carbon dioxide concentration up to 40% and equivalence ratio ranges from 0.7 to 1.4. The results showed that low laminar burning velocity exist at high pressure. Burning velocity increased with temperature decreased with CO2 addition.

In biogas fuelled HCCI engine, and to increase operating range, Iván D. Bedoya et al. [4] have studied experimentally three parameters: oxygen enrichment, gasoline pilot port injection and delayed combustion time. Results showed that oxygen content in air above 27% combined with higher inlet absolute pressure lead to more stabilized combustion at low equivalence ratios. Gasoline pilot port injection strongly improved auto-ignition properties of biogas/air mixture and decreased HC and CO emissions at low load limit. Delayed combustion within certain limits increased IMEPg (gross Indicated Mean Effective Pressure) and reduced ringing intensities.

Stability of turbulent non-premixed biogas flame for turbomachinery applications under a wide range of coflow, swirl and burner geometry was examined experimentally by Saediamiri et al. [5]. A well-defined region within which a stable lifted biogas flame can operate safely was identified.

The aim of the present study is to investigate biogas diffusion flame structure and emissions in counterflow configuration over a wide range of operating conditions (CO2/CH4 molar ratio between 0.33 and 1.5 and ambient pressure from 1 to 10 atm). A special emphasis is put on chemical and thermal effect of CO2.

2. The laminar flamelet model

The counterflow flame (figure 1) is analyzed in mixture fraction space using flamelet approach. Air formed by oxygen and nitrogen is injected from the first side, while biogas composed by methane and carbon dioxide is injected by the second side. A thin sheet of flame is formed between the injectors.

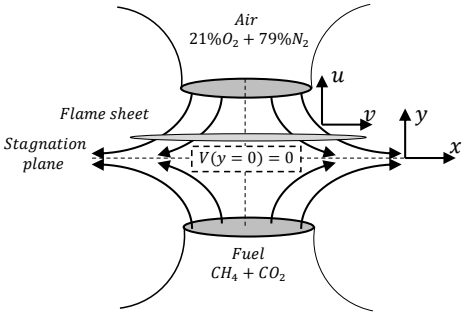

Figure 1: Counter-flow configuration of biogas diffusion flame

Considering Z direction perpendicular to flame sheet, Z stands for the mixture fraction which takes the value 1 in the fuel stream and 0 in the oxidizer one. Flamelet equations simplifies to [6]:

$$\rho\frac{\partial Y_i}{\partial t}=\frac{1}{2}\rho\chi\frac{1}{Le_i}\frac{\partial^2 Y_i}{\partial Z^2}+\dot{\omega}_i-\frac{1}{2}\frac{\partial Y_i}{\partial Z}\left[\frac{1}{2}\left(1-\frac{1}{Le_i}\right)\left(\frac{\partial\rho\chi}{\partial Z}+\rho\chi\frac{C_p}{\lambda}\frac{\partial\left(\frac{\lambda}{C_p}\right)}{\partial Z}\right)\right] \quad (1)$$

$$\rho\frac{\partial T}{\partial t}=\frac{1}{2}\rho\chi\frac{\partial^2 T}{\partial Z^2}-\frac{1}{C_p}\sum_i H_i\dot{\omega}_i+\frac{1}{2c_p}\rho\chi\left[\frac{\partial C_p}{\partial Z}+\sum_i\frac{1}{Le_i}c_{p,i}\frac{\partial Y_i}{\partial Z}\right]\frac{\partial T}{\partial Z}-\frac{1}{C_p}\left[4\sigma p\sum_j X_j a_i\left(T^4-T_b^4\right)\right] \quad (2)$$

Notation in Equations (1) and (2) is as follows: Yi, T, ρ are the ith species mass fraction, temperature and density, respectively.Leiis the Lewis number of the ith species defined as $Le=\lambda/(\rho D_{im}C_p)$ where Dimis the multi-component ordinary diffusion coefficient, $\dot{\omega}_i$is the ith species reaction rate and χ is the instantaneous scalar dissipation rate defined by: $\chi=2D_z(\nabla Z.\nabla Z)$. Its modelling is based on the relation below which is taken from the counter-flow geometry [7]:

$$\chi=\chi_{st}\frac{\phi}{\phi_{st}}\frac{g(Z)}{g(Z_{st})} \quad (3)$$

$\chi_{st}$is the scalar dissipation rate at stoichiometry and ϕ is a factor introduced in order to include density variation effect [8]:

$$\phi=\frac{1}{4}\frac{3\left(\sqrt{\rho_\infty/\rho}+1\right)^2}{2\sqrt{\rho_\infty/\rho}+1} \quad (4)$$

The subscript ∞ means the oxidizer stream.

The function $g(Z)$ is given as follows [9] :

$$g(Z)=\exp\left[-2\left(\mathrm{erfc}^{-1}(2Z)\right)^2\right] \quad (5)$$

where erfc^{-1} is the inverse of the complementary error function.

Thestoichiometric dissipation scalar is found from :

$$\chi_{st}=\frac{a}{\pi}\exp\left[-2\left(\mathrm{erfc}^{-1}(2Z_{st})\right)^2\right] \quad (6)$$

Where a is the strain rate.

The stoechiometric mass fraction is given by :

$$Z_{st}=\frac{1}{1+sY_{FF}/Y_{OO}} \quad (7)$$

Where s is the stoechiometric mass ratio of oxygen to fuel, Y_{FF} and Y_{OO} are the feed stream mass fraction of the fuel (regardless of the chemical composition) and oxygen, respectively.

The two parameters are to input in equations (1) and (2), mixture fraction Z and stoichiometric scalar dissipation rate χst.

3. Simulation details

The flamelet equations (1) and (2) are solved for several values of CO2/CH4 molar ratio until steady state is achieved assuming Lei = 1 for all species involved in the chemical mechanism. Calculations are carried out with PrePDF 4 code [10]. Computations are performed over a wide range of CO2/CH4

molar ratio (0.33 to 1.5) and ambient pressure (from 1 atm to 10 atm). Hereafter results are presented for two biogases composition, BG40 (40% CO2 and 60%CH4) and BG60 (60% CO2 and 40% CH4). Biogas oxidation chemistry is modelledby the GRI Mech-3.0 mechanism that involves 53 species and 325 reactions. Chemical and thermal influences of biogas CO2 content are evaluated over the range of operating conditions considered using an artificial non reacting species X which has the same thermal and transport properties as CO2 [11].

4. Results and Discussion

In this section, computations results are presented for each operating parameter.

4.1 Biogas composition effects

Biogas composition effect on flame structure and NO emission is investigated at χ=20 s-1and P = 1 atm. An analysis of thermal and chemical effect of CO2 is also provided. CO2 volume content is increased from 25% to 60%. These limits correspond to low quality biogas, which contains a small amount of methane, and a high quality one containing important quantities of methane. First, results of adiabatic flame temperature are shown followed by flame structure and NO emission. An analysis of thermal and chemical effect of CO2 addition is then provided.

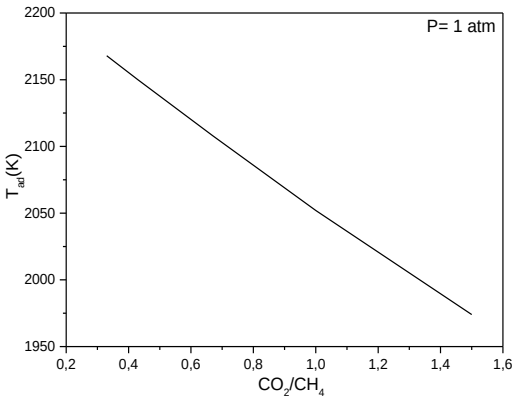

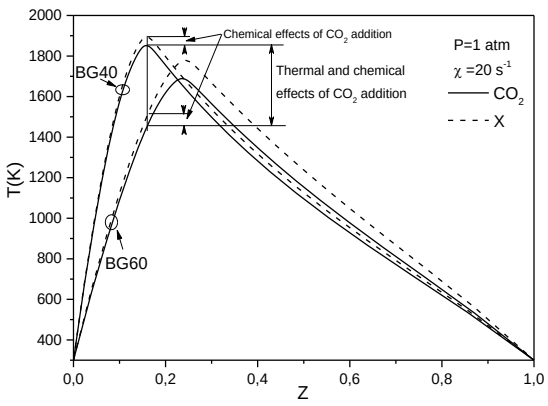

Figure 2: Adiabatic flame temperatureFigure 3: Flame temperature

Figure 2 depicts the influence of CO2/CH4 molar ratio on adiabatic flame temperature which is obtained from thermodynamic equilibrium calculation. Adiabatic flame temperature deceases linearly with CO2/CH4 ratio. More CO2 is added, the smaller is the power input.

Figures 3 to8 present flame structures and NO emission at χ=20 s-1. Inlet temperature and ambient pressure are 300 K and 1 atm, respectively. Flame structure includes distributions of flame temperature, mass fractions of major species(H2O, CO2 and CO) and minor species (OH).

According to these figures, CO2 addition induces a shift of the radial spreading profiles of the involved temperature and species towards the fuel side. This is due to low diffusivity and heaviness of CO2. Indeed, reducing the concentration of CH4 increases the stoichiometric mixture fraction and this

displaces all temperature and species mass fraction curves to the right.

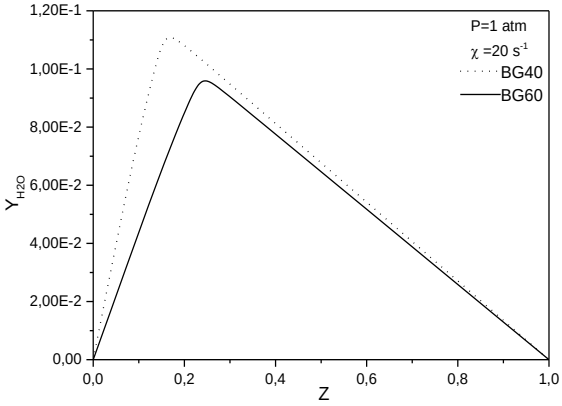

Figure 4: H_2O mass fraction

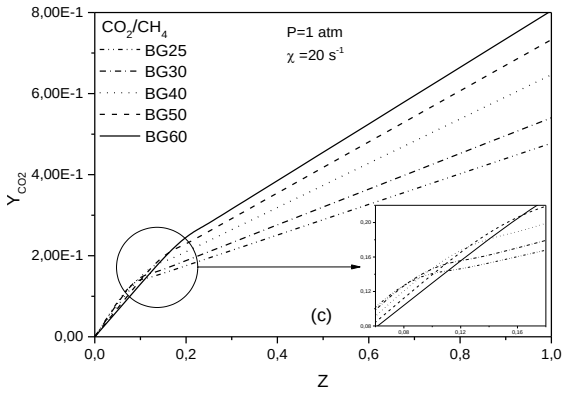

Figure 5: CO_2 mass fraction

The maximum temperature (figure 3) decreases with CO2/CH4 ratio and occurs at the rich side of the stoichiometric mixture fraction of the biogas mixtures. Forboth BG40 and BG60 biogases, chemical and thermal CO2 addition effects are shown. The flame produces less H2O (figure 4) and slightly less CO2 for Z < 0.12 and more CO2 for Z > 0.12 (figure 5).CO mass fraction is lowered with CO2 addition(figure 6).

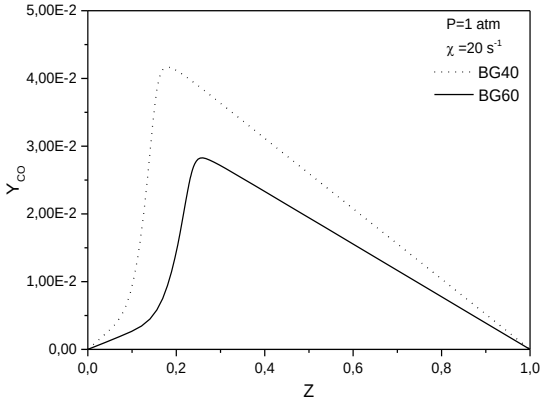

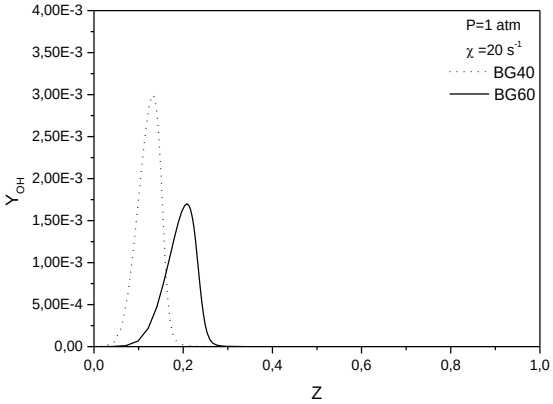

Figure 6: CO mass fractionFigure 7: OH mass fraction

CO2in the fuel mixture rise reduces the mass fraction of OH radical(figure 7).The same behavior has been found in previous studies [12].

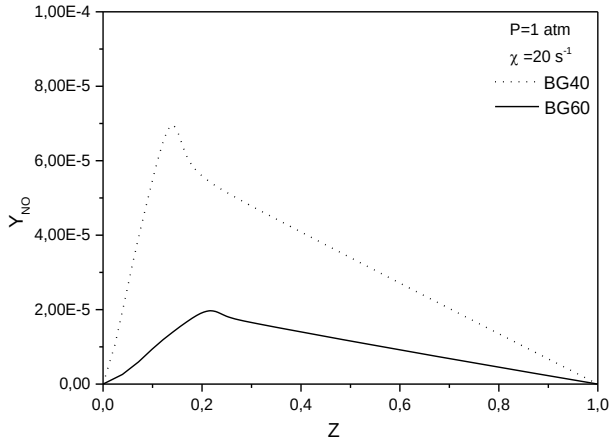

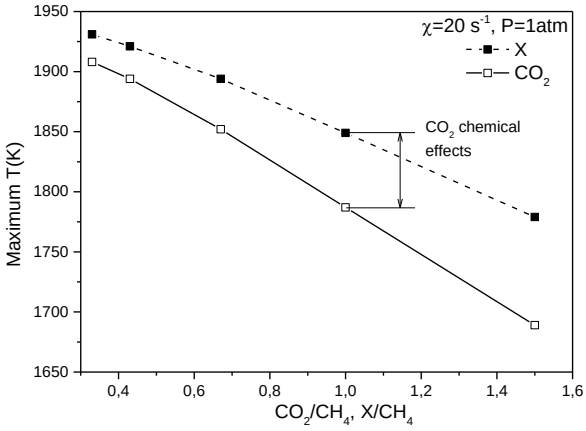

Figure 8: NO mass fractionFigure 9: Maximum flame temperature

NO mass fraction (figure 8) is maximal at temperature peaks, located at z_{st}, it decreases due to reduction of reactive species with increasing CO_2/CH_4 molar ratio.

Figures 9 and 10 illustrate chemical effects of CO_2 addition on maximum temperature and maximum NO species for different CO_2/CH_4 molar at ambient pressure of 1 atm and scalar dissipation of 20 s^{-1}.

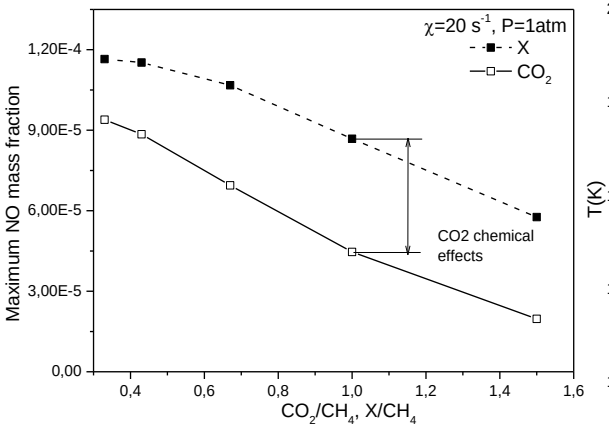

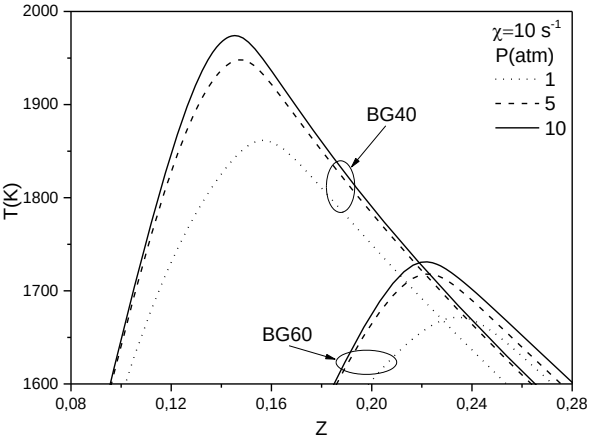

Figure 10: Maximum NO mass fractionFigure 11: Flame temperature

From figure 9,it can be seen that both chemical and thermal effects of CO_2 addition reduce maximum flame temperature; it is worth noting that chemical effect is more pronounced with increasing CO_2/CH_4 molar ratio.In figure 10, maximum NO mass fraction isalso decreased by thermal and chemical CO_2 effects.

4.2 Pressure effects

Pressure effect results are presented for BG40 and BG60 biogases, scalar dissipation of 10 s^{-1} and ambient pressure from 1 to 10 atm.

Effect of ambient pressure on flame temperature, H_2O, CO_2, CO, OH and NO mass fractions arecharacterized in figures 11 to 16.

Figure 11 shows that with increasing pressure, flame reaction zone become thinner [14], as can be seen in temperature and species profiles. Flame thickness is proportional to $(Pa)^{-1/2}$ since it is of the order of $(D/a)^{1/2}$ and D is inversely proportional to pressure, where D is the mixture diffusion coefficient and $a$is the strain rate[25]. According to this, thermal radiation becomes progressively less important since it is inherently a volumetric phenomenon.

Pressure rise increases flame temperature (figure 11) and CO_2 mass fraction (figure 13).This increase is fast from 1 to 5 atm and more gradual between 5 and 10 atm [15]. Pressure effect is more visible on BG40 than BG60 biogas, peak temperature difference and deflection in CO_2 profile are important in BG40 compared with BG60. However, H_2O mass fraction (figure 12) is less sensitive to pressure increase for both biogases; its variation is very slight.

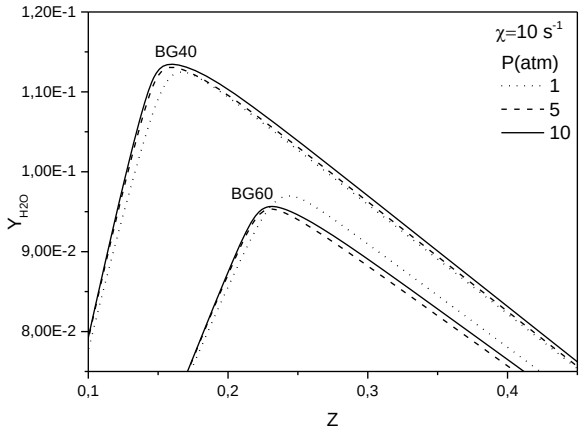

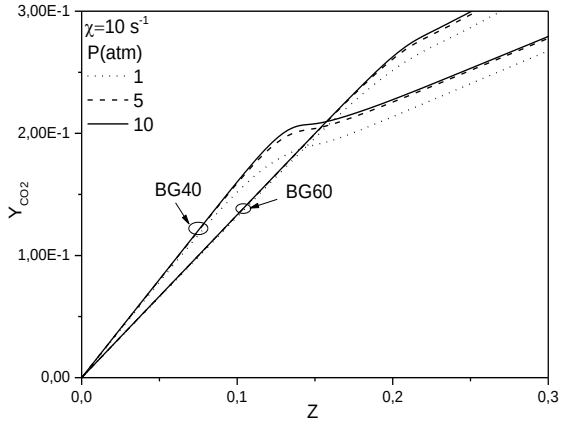

Figure 12: H_2O mass fractionFigure 13: CO_2 mass fraction

CO mass fraction (figure 14) is deceased with pressure; this decrease is fast from 1 to 5 atm and more gradual between 5 and 10 atm.

OH and NO mass fractions (figures 15 and 16) are all reduced with pressure rise. The chain branching reaction are inhibited by produced hydrocarbon products induced with CO_2 addition, furthermore high pressure promotes recombination reactions involving a third body. This reduces the chain branching and then CO and NO mass fractions.

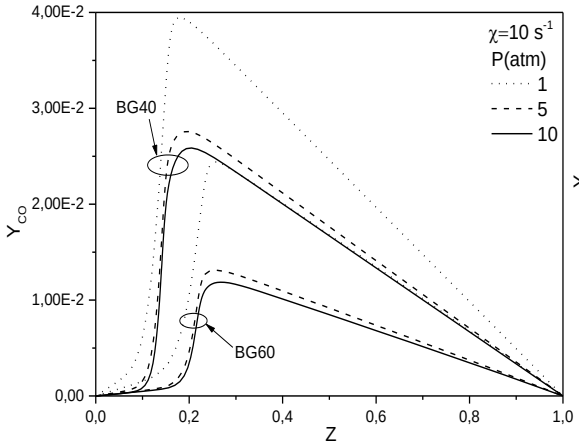

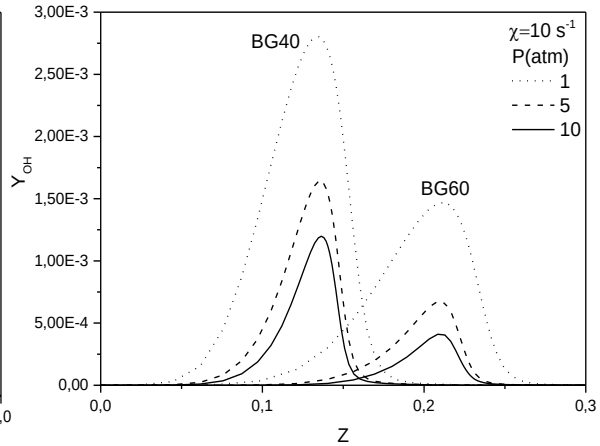

Figure 14: CO mass fractionFigure 15: OH mass fraction

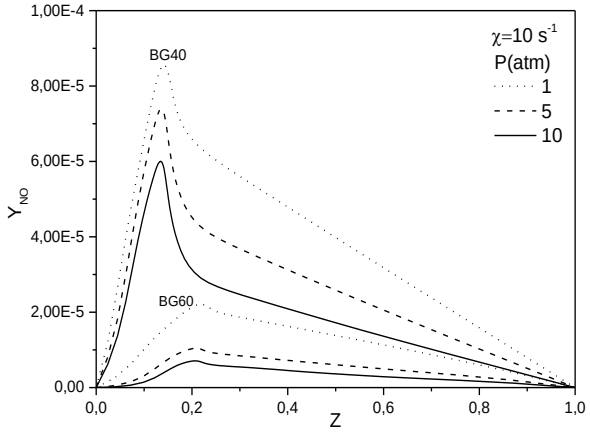

Figure 16: NO mass fraction

From figure 17,it can be seen that the maximum temperature is decreased by CO_2 chemical effects and augmented by pressure. Figure 18 shows that maximum NO mass fraction diminishes with CO_2 chemical effects and pressure rise.

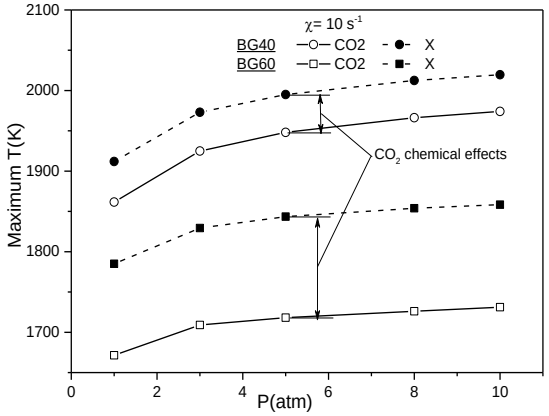

Figure 17: Maximum flame temperature

3.3 NO emissions

The emission index, EINO, is a global parameter that has been commonly used to characterize NO emission from different flames. It is defined according to [31]:

$$EINO = \frac{\int W_{NO}\dot{w}_{NO}dz}{\int W_{fuel}\dot{w}_{fuel}dz}$$

Where W_i and $\dot{w}_i$ are molecular weights and molar production rates of ith species, respectively.

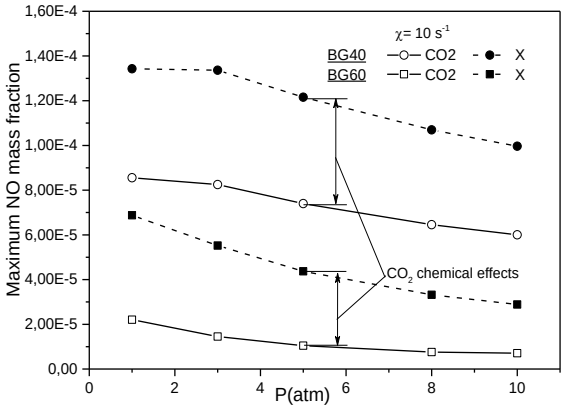

Figure 18: Maximum NO mass fraction

Figures 19 and 20show that pressure and CO_2 mass fraction rise reduce the NO emissions index.

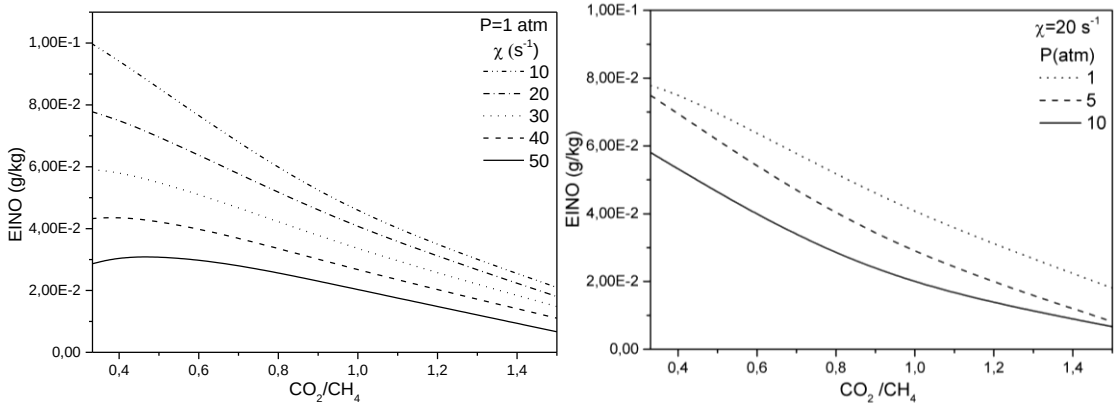

Figure 19: EINO distribution with concentrationFigure 20: EINO distribution with pressure

4. Conclusion

A numerical study on flame structure and emissions of biogas counter-flow diffusion flame was conducted in mixture fraction space over a wide range of operating conditions: CO_2 volume in the fuel mixture ranging from 25 to 75% and ambient pressure from 1 to 10 atm. Thermal and chemical effects of CO_2 addition on flame structure were also investigated. The following conclusions can be drawn

- Flame temperature is decreased by both thermal and chemical CO_2 addition effects. Also, radiation losses are enhanced with CO_2 enrichment.
- Maximum mass fraction of chain carrier radicals and NO are decreased by CO_2 chemical effect and increased by CO_2/CH_4 molar ratio.
- NO emission index is reduced with CO_2 addition in the whole composition and strain rate space.
- Added CO_2 amount more than a digestible one plays a role of diluent and limits chemical reaction participation.
- The chain branching reaction is inhibited with CO_2 addition and recombination reactions are promoted at high pressure, as a result CO and NO mass fractions are reduced.

References

[1] X. Paubel,A. Cessou,D. Honore,L. Vervisch,R. Tsiava, A flame stability diagram for piloted non-premixed oxycombustion of low calorific residual gases Proceedings of the Combustion Institute, Volume 31, Issue 2, January 2007, Pages 3385–3392

[2] Saeed Jahangirian; Abraham Engeda; Indrek S. Wichman, Thermal and chemical structure of biogas counterflow diffusion flames, Energy and Fuels. 2009;23(11):5312-5321.

[3] Nathan Hinton; Richard Stone**,**Laminar burning velocity measurements of methane and carbon dioxide mixtures (biogas) over wide ranging temperatures and pressures**,** Fuel 116(2014) 743-750

[4] Iván D. Bedoya ,Samveg Saxena,Francisco J. Cadavid,Robert W. Dibble,Martin Wissink, Experimental evaluation of strategies to increase the operating range of a biogas-fueled HCCI engine for power generation, Applied EnergyVolume 97, September 2012, Pages 618–629

[5] Meghdad Saediamiri, Madjid Birouk, Janusz A. Kozinski**,** On the stability of a turbulent non-premixed biogas flame: Effect of low swirl strength**,**Combustion and Flame 01/2014; 161(5):1326–1336

[6]N. Peters, Turbulent combustion, Cambridge University Press, 2000.

[7]H. Pitsch ,N. Peters, A Consistent Flamelet Formulation for Non-Premixed Combustion Considering Differential Diffusion Effects, Combustion and FlameVolume 114, Issues 1–2, July 1998, Pages 26–40

[8] J. S. Kim, F. A. Williams, Extinction of diffusion flames with non-unity Lewis numbers, Journal of Engineering MathematicsApril 1997, Volume 31, Issue 2-3, pp 101-118

[9] N. Peters, Laminar Diffusion Flamelet Models in Non Premixed Combustion, Prog. Energy Combust. Sci., 10:319-339, 1984.

[10] FLUENT Inc., Fluent User's Guide Ver. 6.2. (2005).

[11] Jeong Park, Dong-Jin Hwang, Jong-Geun Choi, Kee-Man Lee, Sang-In Keel and Sung-Hoon Shim, Chemical effects of CO2 addition to oxidizer and fuel streams on flame structure in H2–O2 counterflow diffusion flames, Int. J. Energy Res. 2003; 27:1205–1220

[21] A. Matynia, J. Molet, C. Roche, M. Idir, S. de Persis, L. Pillier, Measurement of OH concentration profiles by laser diagnostics and modeling in high-pressure counterflow premixed methane/air and biogas/air flames,Combustion and FlameVolume 159, Issue 11, November 2012, Pages 3300–3311

[22] Hsin-Yi Shih , Jou-Rong Hsu, A computational study of combustion and extinction of opposed-jet syngas diffusion flames, International Journal of Hydrogen EnergyVolume 36, Issue 24, December 2011, Pages 15868–15879

[14] U. Niemann, K. Seshadri, F.A. Williams, Effect of pressure on structure and extinction of near-limit hydrogen counterflow diffusion flames, Proceedings of the Combustion Institute 01/2013; 34(1):881-886

[15] K. Safer, F. Tabet, A. Ouadha, M. Safer and I. Gökalp, Simulation of a syngas counter-flow diffusion flame structure and NO emissions in the pressure range 1 - 10 atm, Fuel Processing TechnologyVolume 123, July 2014, Pages 149–158.

[16] X.L. Zhu, J.P. Gore, Radiation effects on combustion and pollutant emissions of high-pressure opposed flow methane/air diffusion flames, Combustion and FlameVolume 141, Issues 1–2, April 2005, Pages 118–130